Decoherence of quantum registers

John H. Reina,[1,*] Luis Quiroga,[2,†] and Neil F. Johnson[1,‡]
[1]*Physics Department, Clarendon Laboratory, Oxford University, Oxford, OX1 3PU, United Kingdom*
[2]*Departamento de Física, Universidad de los Andes, A.A. 4976, Bogotá, Colombia*
(Received 8 May 2001; revised manuscript received 19 July 2001; published 1 March 2002)

The dynamical evolution of a quantum register of arbitrary length coupled to an environment of arbitrary coherence length is predicted within a relevant model of decoherence. The results are reported for quantum bits (qubits) coupling individually to different environments (''independent decoherence'') and qubits interacting collectively with the same reservoir (''collective decoherence''). In both cases, explicit decoherence functions are derived for any number of qubits. The decay of the coherences of the register is shown to strongly depend on the input states: We show that this sensitivity is a characteristic of *both* types of coupling (collective and independent) and not only of the collective coupling, as has been reported previously. A nontrivial behavior (''recoherence'') is found in the decay of the off-diagonal elements of the reduced density matrix in the specific situation of independent decoherence. Our results lead to the identification of decoherence-free states in the collective decoherence limit. These states belong to subspaces of the system's Hilbert space that do not get entangled with the environment, making them ideal elements for the engineering of ''noiseless'' quantum codes. We also discuss the relations between decoherence of the quantum register and computational complexity based on the dynamical results obtained for the register density matrix.

DOI: 10.1103/PhysRevA.65.032326 PACS number(s): 03.65.Yz, 42.50.Lc, 03.67.−a, 03.67.Lx

I. INTRODUCTION

When any open quantum system, for example, a quantum computer, interacts with an arbitrary surrounding environment, there are two main effects that have to be considered when examining the temporal evolution. First, there is an expected loss of energy of the initial system due to its relaxation, which happens at the rate τ_{rel}^{-1} where τ_{rel} is the relaxation time scale of the system. Second, there is a process that spoils the unitarity of the evolution, the so-called decoherence [1], where the continuous interaction between the quantum computer and the environment leads to unwanted correlations between them in such a way that the computer loses its ability to interfere, giving rise to wrong outcomes when executing conditional quantum dynamics. This phenomenon is characterized by a time that defines the loss of unitarity (i.e., the departure of coherence from unity), the decoherence time τ_{dec}. Usually, the time scale for this effect to take place is much smaller than the one for relaxation, hence quantum computers are more sensitive to decoherence processes than to relaxation ones. For practical applications in quantum computing there are several different systems that might provide a long enough τ_{rel}; however, what really matters for useful quantum information processing tasks (e.g., quantum algorithms) to be performed reliably is the ratio τ_{gating}/τ_{dec}. τ_{gating}, the time required to execute an elementary quantum logic gate, must be much smaller than τ_{dec}. As a rough estimate, fault-tolerant quantum computation has been shown to be possible if the ratio τ_{gating} to τ_{dec} of a single qubit is of the order of 10^{-4} [2] (a qubit is a two-state quantum system, the basic memory cell of any quantum information processor).

Decoherence and quantum theory are unavoidably connected. Indeed, the ubiquitous decoherence phenomenon has been ultimately associated with the ''frontiers'' between the quantum behavior of microscopic systems and the emergence of the classical behavior observed in macroscopic objects [1]: roughly speaking, the decoherence time τ_{dec} determines the energy and length scales at which quantum behavior is observed. It generally depends non-trivially on several different factors such as temperature, dimensionality, quantum vacuum fluctuations, disorder, and others whose origins are less well known (hardware characteristics). The time scale for decoherence depends on the kind of coupling between the system under consideration and the environment, in a range that can go from *pico*seconds in excitonic systems [3] up to *minutes* in nuclear-spin systems [4].

The discovery of algorithms for which a computer based on the principles of quantum mechanics [5] can beat any traditional computer, has triggered intense research into realistic controllable quantum systems. Among the main areas involved in this active research field are ion traps [6], nuclear magnetic resonance [7], quantum electrodynamics cavities [8], Josephson junctions [9], and semiconductor quantum dots [10]. The main challenge that we face is to identify a physical system with appropriate internal dynamics and corresponding external driving forces which enables one to selectively manipulate quantum superpositions and entanglements. For this to be done, the candidate system should have a sufficiently high level of isolation from the environment: quantum information processing will be a reality when optimal control of quantum coherence in noisy environments can be achieved. The various communities typically rely on different hardware methodologies, and so it is important to clarify the underlying physics and limits for each type of physical realization of quantum information processing sys-

*Electronic address: j.reina-estupinan@physics.ox.ac.uk
†Electronic address: lquiroga@uniandes.edu.co
‡Electronic address: n.johnson@physics.ox.ac.uk

tems. As mentioned above, these limits are mainly imposed by the decoherence time of each particular system. However, theoretical work has shown that, in addition to quantum error correcting codes [11,12], there are two additional ways that may potentially lead to decoherence-free or decoherence-controlled quantum information processing: one of them is the so-called ''error avoiding'' approach where, for a given decoherence mechanism (e.g., collective decoherence, discussed below), the existence of ''decoherence-free'' subspaces within the system's Hilbert space can be exploited in order to obtain a quantum dynamics where the system is effectively decoupled from the environment [13,15]. This approach requires the system-environment coupling to possess certain symmetry properties. The other approach is based on ''noise suppression'' schemes, where the effects of unwanted system-bath interactions are dynamically controlled using a sequence of ''tailored external pulses'' [16,17]. These strategies have motivated much theoretical and experimental work. In particular, there are some recent experimental results regarding the engineering of decoherence-free quantum memories [18,19].

We devote this paper to the study of decoherence of an arbitrary quantum register (QR) of L qubits. In addition to providing a general theoretical framework for studying decoherence, we examine in detail the two limits where the qubits are assumed to couple (i) independently and (ii) collectively to an external (bosonic) reservoir. The reservoir is modelled by a continuum of harmonic modes. In Sec. II, we show that the decoherence process is very sensitive to the input states of the register and give explicit expressions for the coherence decay functions. We have found that these functions possess a behavior, which we label ''recoherence'' (or coherence revivals) in the specific case of independent decoherence. This behavior depends strongly on the temperature and the strength of the qubit-bath coupling. By contrast, for a certain choice of the QR input, the calculation of the reduced density matrix leads to the identification of decoherence-free quantum states [13,15], when the qubits are coupled ''collectively'' to the environment, i.e., when the distance between qubits is much smaller than the bath coherence length, and hence, the environment couples in a permutation-invariant way to all qubits. The calculations in this paper were motivated by the results of Refs. [20,21]. The present paper shows that some subtle but important details of these earlier results are incomplete. Particularly, the calculation of the L-QR density matrix reported here leads both to qualitative results, when analyzing the behavior of coherence decay, and quantitative results, when estimating typical decoherence times: these results emerge for $L>1$, as discussed in Sec. III. Concluding remarks are given in Sec. IV. We emphasize that the results of this paper are not restricted to a particular physical system; they are valid for any choice of the qubit system (e.g., photons, atoms, nuclei with spin half, etc.) and any bosonic reservoir.

II. INDEPENDENT VERSUS COLLECTIVE DECOHERENCE

Let us consider the general case of a L-QR coupled to a quantized environment modelled as a continuum of field modes with corresponding creation (annihilation) bath operator $b^\dagger$ (b). Throughout this paper, we will analyze pure dephasing mechanisms only. We will not consider relaxation mechanisms where the QR exchanges energy with the environment leading to bit-flip errors. Hence, the nth qubit operator $J^n \equiv J_z^n$ $(J_x^n = J_y^n = 0)$ [23]. As mentioned earlier, this is a reasonable approach since decoherence typically occurs on a much faster time scale than relaxation. The dynamics of the qubits and the environment can be described by a simplified version of the widely studied spin-boson Hamiltonian [22]

$$H = \sum_{n=1}^{L} \epsilon_n J_z^n + \sum_{\mathbf{k}} \epsilon_{\mathbf{k}} b_{\mathbf{k}}^\dagger b_{\mathbf{k}} + \sum_{n,\mathbf{k}} J_z^n (g_{\mathbf{k}}^n b_{\mathbf{k}}^\dagger + g_{\mathbf{k}}^{n*} b_{\mathbf{k}}), \quad (1)$$

where the first two terms describe the free evolution of the qubits and the environment, and the third term accounts for the interaction between them. Here, $g_{\mathbf{k}}^n$ denotes the coupling between the nth qubit and field modes, which in general depends on the physical system under consideration. The initial state of the whole system is assumed to be $\rho^S(0) = \rho^Q(0) \otimes \rho^B(0)$ (the superscripts stand for system, qubits, and bath), i.e., the QR and the bath are initially decoupled [24]. We also assume that the environment is initially in thermal equilibrium, a condition that can be expressed as

$$\rho^B(0) = \prod_{\mathbf{k}} \rho_{\mathbf{k}}(T) = \prod_{\mathbf{k}} \frac{\exp(-\beta \hbar \omega_k b_{\mathbf{k}}^\dagger b_{\mathbf{k}})}{1 + \langle N_{\omega_k} \rangle}, \quad (2)$$

where $\langle N_{\omega_k} \rangle = [\exp(-\beta \hbar \omega_k) - 1]^{-1}$ is the Bose-Einstein mean occupation number, k_B is the Boltzmann's constant and $\beta \equiv 1/k_B T$. For the model of decoherence presented here, it is clear that we are in a situation where the qubit operator J_z^n commutes with the total Hamiltonian H and therefore, there is no exchange of energy between qubits and environment, as expected. We will not attempt to perform a group-theoretic description for the study of quantum noise control [25]. Instead, we study the specific real-time dynamics of the decay in the QR-density-matrix coherences within the model given by the Hamiltonian Eq. (1) (i.e., Abelian noise processes, in the language of Refs. [26,27]).

In the interaction picture, the quantum state of the combined (qubits plus bath) system at time t is given by $|\Psi(t)\rangle_I = U_I(t)|\Psi(0)\rangle$, where $|\Psi(0)\rangle$ is the initial state of the system, $U_I(t)$ is the time evolution operator, $U_I(t) = T \exp[-i/\hbar \int_o^t H_I(t')dt]$, and T is the time ordering operator. For the Hamiltonian (1), we introduce the notation $H = H_0 + V$, where $H_0 = \Sigma_{n=1}^L \epsilon_n J_z^n + \Sigma_{\mathbf{k}} \epsilon_{\mathbf{k}} b_{\mathbf{k}}^\dagger b_{\mathbf{k}}$ denotes the free evolution term and $V = \Sigma_{n,\mathbf{k}} J_z^n (g_{\mathbf{k}}^n b_{\mathbf{k}}^\dagger + g_{\mathbf{k}}^{n*} b_{\mathbf{k}})$ is the interaction term. Hence, the interaction picture Hamiltonian is given by $H_I(t) = U_0^\dagger(t) V U_0(t)$, with $U_0 = \exp(-i/\hbar H_0 t)$. A simple calculation gives the result

$$H_I(t) = \sum_{n,\mathbf{k}} J_z^n (g_{\mathbf{k}}^n e^{i\omega_k t} b_{\mathbf{k}}^\dagger + g_{\mathbf{k}}^{*n} e^{-i\omega_k t} b_{\mathbf{k}}), \quad (3)$$

which allows us to calculate the time evolution operator $U_I(t)$. The result is (see Appendix B1 for details)

$$U_I(t)=\exp[i\Phi_{\omega_k}(t)]\exp\left[\sum_{n,\mathbf{k}} J_z^n\{\xi_{\mathbf{k}}^n(t)b_{\mathbf{k}}^\dagger-\xi_{\mathbf{k}}^{*n}(t)b_{\mathbf{k}}\}\right] \tag{4}$$

with

$$\Phi_{\omega_k}(t)=\sum_{n,\mathbf{k}} |J_z^n g_{\mathbf{k}}^n|^2\frac{\omega_k t-\sin(\omega_k t)}{(\hbar\omega_k)^2},$$

$$\xi_{\mathbf{k}}^n(t)=g_{\mathbf{k}}^n\varphi_{\omega_k}(t)\equiv g_{\mathbf{k}}^n\frac{1-e^{i\omega_k t}}{\hbar\omega_k}. \tag{5}$$

This result differs from the one reported in Ref. [20] where the *time-ordering operation for $U_I(t)$ was not performed*. As will become clear later, this correction alters the resulting calculation of Ref. [20], and hence changes the results for the reduced density matrix of an arbitrary L-QR. Based on the time evolution operator of Eq. (4), we report here a different result for this density matrix and discuss its implications with respect to those of Ref. [20].

Unless we specify the contrary, we will assume that the coupling coefficients $g_{\mathbf{k}}^n(n=1,\ldots,L)$ are *position dependent*, i.e., that each qubit couples individually to a different heat bath, hence the QR decoheres "*independently*." Implications for the "collective" decoherence case will be discussed later. Let us assume that the nth qubit experiences a coupling to the reservoir characterized by

$$g_{\mathbf{k}}^n=g_{\mathbf{k}}\exp(-i\mathbf{k}\cdot\mathbf{r}_n), \tag{6}$$

where $\mathbf{r}_n$ denotes the position of the nth qubit. It is easy to see that the unitary evolution operator given by Eq. (4) produces entanglement between register states and environment states [20]. The degree of the entanglement produced will strongly depend on the qubit input states and also on the separation $||\mathbf{r}_m-\mathbf{r}_n||$ between qubits because of the position-dependent coupling. As we will show later, for some kind of input states, no decoherence occurs at all despite the fact that all of the qubits are interacting with the environment. We will also identify states with dynamics decoupled from thermal fluctuations; this fact may be relevant when designing experiments where the involved quantum states have dephasing times (mainly due to temperature-dependent effects) on a very short time scale, as in the solid state, for example. We will also see that the above features are key issues when proposing schemes for maintaining coherence in quantum computers [13].

Due to the pure dephasing (i.e., Abelian) characteristic of the noise model considered here, we can calculate analytically the functional dependence of the decay of the coherences of the QR by taking into account all the field modes of the quantized environment. We shall follow the notation of Ref. [20]. Let us consider the reduced density matrix of the L-QR: the matrix elements of this reduced operator can be expressed as

$$\rho^Q_{\{i_n,j_n\}}(t)=\langle i_L,i_{L-1},\ldots,i_1|\mathrm{Tr}_B\{\rho^S(t)\}|j_L,j_{L-1},\ldots,j_1\rangle, \tag{7}$$

where $\{i_n,j_n\}\equiv\{i_1,j_1;i_2,j_2;\ldots;i_L,j_L\}$ refers to the qubit states of the QR and

$$\rho^S(t)=U_I(t)\rho^Q(0)\otimes\rho^B(0)U_I^\dagger(t). \tag{8}$$

From this expression it becomes clear that the dynamics of the register is completely determined by the evolution operator $U_I(t)$. In Eq. (8), the initial density matrix of the register can be expressed as $\rho^Q(0)=\rho^Q_{i_1,j_1}(0)\otimes\rho^Q_{i_2,j_2}(0)\otimes\ldots\otimes\rho^Q_{i_L,j_L}(0)$, where $\rho^Q_{i_n,j_n}=|i_n\rangle\langle j_n|$. In this expansion, $|i_n\rangle=|\pm\frac{1}{2}\rangle$ are the possible eigenstates of J_z^n and will be associated with the two level qubit states $|1\rangle$ and $|0\rangle$, respectively. The eigenvalues $i_n=\pm\frac{1}{2}$ and $j_n=\pm\frac{1}{2}$. In what follows, the subscripts of Eq. (7) will be renamed with the values one and zero to indicate the actual values $\frac{1}{2}$ and $-\frac{1}{2}$, respectively. Hence, we can rewrite Eq. (7) as

$$\rho^Q_{\{i_n,j_n\}}(t)=\mathrm{Tr}_B[\rho^B(0)U_I^{\dagger\{j_n\}}(t)U_I^{\{i_n\}}(t)]\rho^Q_{\{i_n,j_n\}}(0), \tag{9}$$

$$U_I^{\{i_n\}}(t)\equiv\exp\left[i\sum_{\mathbf{k}}|g_{\mathbf{k}}|^2 s(\omega_k,t)\sum_{m,n}e^{i\mathbf{k}\cdot\mathbf{r}_{mn}}i_m i_n\right]\times\exp\left[\sum_{n,\mathbf{k}}\{g_{\mathbf{k}}\varphi_{\omega_k}(t)i_n e^{-i\mathbf{k}\cdot\mathbf{r}_n}b_{\mathbf{k}}^\dagger - g_{\mathbf{k}}^*\varphi_{\omega_k}^*(t)i_n e^{i\mathbf{k}\cdot\mathbf{r}_n}b_{\mathbf{k}}\}\right], \tag{10}$$

and calculate explicitly the decay of the coherences for the L-QR. The result is (see Appendix B2)

$$\begin{aligned}\rho^Q_{\{i_n,j_n\}}(t)=&\exp\left[-\sum_{\mathbf{k};m,n}|g_{\mathbf{k}}|^2c(\omega_k,t)\times\coth\left(\frac{\hbar\omega_k}{2k_BT}\right)(i_m-j_m)(i_n-j_n)\cos\mathbf{k}\cdot\mathbf{r}_{mn}\right]\\&\times\exp\left[i\sum_{\mathbf{k};m,n}|g_{\mathbf{k}}|^2s(\omega_k,t)(i_m i_n-j_m j_n)\cos\mathbf{k}\cdot\mathbf{r}_{mn}\right]\\&\times\exp\left[-2i\sum_{\mathbf{k};m,n}|g_{\mathbf{k}}|^2c(\omega_k,t)i_m j_n\sin\mathbf{k}\cdot\mathbf{r}_{mn}\right]\\&\times\rho^Q_{\{i_n,j_n\}}(0),\end{aligned} \tag{11}$$

where $\mathbf{r}_{mn}\equiv\mathbf{r}_m-\mathbf{r}_n$ is the relative distance between the mth and nth qubits, $s(\omega_k,t)=[\omega_k t-\sin(\omega_k t)]/(\hbar\omega_k)^2$, and $c(\omega_k,t)=[1-\cos(\omega_k t)]/(\hbar\omega_k)^2$. In the continuum limit, Eq. (11) reads

$$\rho^Q_{\{i_n,j_n\}}(t)=\exp[i\{\Theta_d(t,t_s)-\Lambda_d(t,t_s)\}]\times\exp[-\Gamma_d(t,t_s;T)]\rho^Q_{\{i_n,j_n\}}(0), \tag{12}$$

where

$$\Theta_d(t,t_s)=\int d\omega\ I_d(\omega)s(\omega,t) \times 2\sum_{\substack{m=1,n=2\\ m\neq n}}^{L}(i_m i_n - j_m j_n)\cos(\omega t_s), \quad (13)$$

$$\Lambda_d(t,t_s)=2\int d\omega\ I_d(\omega)c(\omega,t)\sum_{\substack{m=1\\ n=2}}^{L} i_m j_n \sin(\omega t_s), \quad (14)$$

and

$$\Gamma_d(t,t_s;T)=\int d\omega\ I_d(\omega)c(\omega,t)\coth\left(\frac{\omega}{2\omega_T}\right) \times\left\{\sum_{m=1}^{L}(i_m-j_m)^2+2\sum_{\substack{m=1,n=2\\ m\neq n}}^{L}(i_m-j_m) \times(i_n-j_n)\cos(\omega t_s)\right\}. \quad (15)$$

Here, $\omega_T\equiv k_B T/\hbar$ is the thermal frequency (see discussion below), $\omega t_s\equiv \mathbf{k}\cdot\mathbf{r}_{mn}$ sets the "*transit time*" t_s, and $I_d(\omega)\equiv\Sigma_{\mathbf{k}}\delta(\omega-\omega_{\mathbf{k}})|g_{\mathbf{k}}|^2\equiv(dk/d\omega)G(\omega)|g(\omega)|^2$ is the spectral density of the bath. This function is characterized by a cutoff frequency ω_c that depends on the particular physical system under consideration and sets $I_d(\omega)\mapsto 0$ for $\omega\gg\omega_c$ [22]. We see that an explicit calculation for the decay of the coherences requires the knowledge of the spectral density $I_d(\omega)$. Here, we assume that $I_d(\omega)=\alpha_d\omega^d e^{-\omega/\omega_c}$ [22], where d is the dimensionality of the field and $\alpha_d>0$ is a proportionality constant that characterizes the strength of the system-bath coupling. Hence, the functional dependence of the spectral density relies on the dimensionality of the frequency dependence of the density of states $G(\omega)$ and of the coupling $g(\omega)$. In Eq. (12), the "transit time" t_s has been introduced in order to express the QR-bath coupling in the frequency domain. This transit time is of particular importance when describing the specific "independent" decoherence mechanism, because of the position-dependent coupling between qubits and bath modes. However, in a scenario where the qubits are coupled "collectively" to the same environment, t_s does not play any role (see below).

The result of Eq. (12) differs in several respects from the one reported in [20]: the decoherence function $\Gamma_d(t,t_s;T)$ contains additional information about the characteristics of the independent decoherence and the way in which the individual qubits couple to the environment through the position-dependent terms which are proportional to $\cos(\mathbf{k}\cdot\mathbf{r}_{mn})$. In essence, this means that the entanglement of the register with the noise field depends on the qubit separation. Also, the expression for $\rho^Q_{\{i_n,j_n\}}(t)$ reveals the dynamical factor $\aleph_d(t,t_s)\equiv\Theta_d(t,t_s)-\Lambda_d(t,t_s)$, which must be taken into account when determining typical decoherence times for the L-QR.

It is interesting that the decoherence effects arising from thermal noise can be separated from the ones due purely to vacuum fluctuations. This is simply because the average number of field excitations at temperature T can be rewritten as $\langle N_\omega\rangle_T=\frac{1}{2}\exp(-\hbar\omega/2k_BT)\mathrm{cosech}(\hbar\omega/2k_BT)$, and hence $\coth(\hbar\omega/2k_BT)=1+2\langle N_\omega\rangle_T$ in Eq. (15). The other term contributing to the decay of the coherences in Eq. (12), $\aleph_d(t,t_s)$, is due purely to quantum vacuum fluctuations. The separation made above allows us to examine the different time scales present in the (QR plus bath) system's dynamics. The fastest time scale of the environment is determined by the cutoff: $\tau_c\sim\omega_c^{-1}$, i.e., τ_c sets the "memory" time of the environment. Hence, the vacuum fluctuations will contribute to the dephasing process only for times $t>\tau_c$. Also note that the characteristic thermal frequency $\omega_T\equiv k_BT/\hbar$ sets another fundamental time scale $\tau_T\sim\omega_T^{-1}$: thermal effects will affect the qubit dynamics only for $t>\tau_T$. Hence, we see that quantum vacuum fluctuations contribute to the dephasing process only in the regime $\tau_c<t<\tau_T$. From this identification it becomes clear that the qubit dynamics and hence the decoherence process of our open quantum system will depend on the ratio of the temperature-to-cutoff parameter ω_T/ω_c and the spectral function $I_d(\omega)$. Later, we will analyze how different qualitative behaviors are obtained for the decoherence depending on the relationship between the cutoff and the thermal frequency. It is worth noticing that the analytical separation between the thermal and vacuum contributions to the overall decoherence process is a convenient property of the pure dephasing (Abelian) model considered here. Further generalizations of this model, e.g., by including relaxation mechanisms, should make this separation nontrivial because the problem becomes no longer exactly solvable.

Next, we analyze the case of "collective decoherence." This situation can be thought of as a bath of "long" coherence length (mean effective wavelength λ) if compared with the separation r_{mn} between qubits, in such a way that $\lambda\gg r_{mn}$, and hence the product of Eq. (6) has $\exp(-i\mathbf{k}\cdot\mathbf{r}_n)\approx 1$. Roughly speaking, we are in a situation where all the qubits "feel" the same environment, i.e., $g^n_{\mathbf{k}}\equiv g_{\mathbf{k}}$. A similar calculation to the one followed in Appendix B gives the following result for the decay of the coherences for the case of collective coupling to the reservoir:

$$\rho^Q_{i_n,j_n}(t)=\exp\left\{i\Theta_d(t)\left[\left(\sum_{m=1}^{L} i_m\right)^2-\left(\sum_{m=1}^{L} j_m\right)^2\right]\right\} \times\exp\left\{-\Gamma_d(t;T)\left[\sum_{m=1}^{L}(i_m-j_m)\right]^2\right\}\rho^Q_{i_n,j_n}(0), \quad (16)$$

where

$$\Theta_d(t)=\int d\omega\ I_d(\omega)s(\omega,t), \quad (17)$$

and

$$\Gamma_d(t;T)=\int d\omega\, I_d(\omega)c(\omega,t)\coth\left(\frac{\omega}{2\omega_T}\right). \qquad (18)$$

Expressions (12) and (16) are to be compared with those reported in Refs. [20] and [21]. Clearly, the result for the evolution operator $U_I(t)$ of Eq. (4) induces a QR-environment dynamics different from the one reported in [20]. This fact has been pointed out in Ref. [21] for the situation of collective decoherence; in this particular case, our results coincide with theirs. However, we obtain different results when considering the situation of independent decoherence: the dynamical factor $\aleph_d(t,t_s)$ includes additional information about individual qubit dynamics that cannot be neglected. Indeed, from the results derived in Ref. [21], the authors argue that the damping of the independent decoherence is insensitive to the type of initial states and hence the sensitivity to the input states is only a property of the collective decoherence. As can be deduced from Eqs. (12) and (16), we find that this statement is not generally true and that the sensitivity to the initial states is a property of both collective *and* independent decoherence. This result is particularly illustrated for the case of a 2-QR in the next section. From the expressions (17) and (18) we see that for $\hbar\omega \ll k_BT$, the high-temperature environment (high-TE), the phase damping factor $\Gamma_d(t;T)$ is the main agent responsible for the qubits' decoherence, while the other dynamical damping factor $\Theta_d(t)$ plays a minor role. In this case ω_c is actually the only characteristic frequency accessible to the system ($\omega_c \ll \omega_T$) and thermal fluctuations always dominate over the vacuum ones. However, when we consider the situation $\omega_c \gg \omega_T$, the low-temperature environment (low-TE), these damping factors compete with each other over the same time scale, and $\Theta_d(t)$ now plays a major role in eroding the qubits' coherence. Here there is a much more interesting dynamic between thermal and vacuum contributions (see next section). This shows the difference and the importance of the additional terms of the reduced density matrix reported here when compared with those of Refs. [20,21]. The above statements will be illustrated in the next section.

So far, the dynamics of the qubits and their coupling to the environment has been discussed in the interaction representation. To go back to the Schrödinger representation, recall $\rho_{Sch}(t)=U_0(t)\rho_I(t)U_0^\dagger(t)$, with $\rho_I(t)$ as calculated before for the qubits decoherence [Eqs. (12) and (16)]. Also, note that in the Schrödinger representation (here denoted with subindex *Sch*) $U_0(t)$ introduces mixing but not decoherence. Next, we consider some particular cases which allow us to evaluate the expressions (12) and (16) and hence give a qualitative picture of the respective decoherence rates for both collective and independent decoherence situations.

III. DIMENSIONALITY OF THE FIELD AND DECOHERENCE RATES FOR FEW-QUBIT SYSTEMS

In this section, we analyze the qualitative behavior of the decay of the coherences given by Eqs. (12) and (16) for single- and two-qubit systems.

A. Single-qubit case

Here, we consider the case of only one qubit in the presence of a thermal reservoir, as defined in Eq. (2). Hence, for both types of coupling [Eqs. (12) and (16)] we get

$$\rho^Q_{i_n,j_n}(t)=\exp[-\Gamma_d(t,T)]\rho^Q_{i_n,j_n}(0). \qquad (19)$$

By using Eq. (4), with $d=1$, it is easy to show that the populations remain unaffected: $\rho^Q_{ii}(t)=\rho^Q_{ii}(0)$, $i=0,1$. In general ($i\neq j$), the decay of coherences is determined by Eq. (19). Here we can identify the main time regimes of decoherence for different dimensionalities of the field. In what follows, we consider the case of reservoirs with both one-dimensional density of states ("Ohmic") and three-dimensional density of states ("super-Ohmic"), i.e., $G(\omega)=\text{const}$ and $G(\omega)=\omega^2$, respectively, where the frequency-dependent coupling $g(\omega)\propto\sqrt{\omega}$, as considered in [20]. From Eq. (19), we see that a general solution for the case $d=1$ requires numerical integration (see Appendix A). However, for the case where the interplay between thermal and vacuum effects is more complex, i.e., the low-TE ($\omega_T \ll \omega_c$), we can solve it analytically. Here we get

$$\Gamma_1(t,T)\approx c_1\left[2\omega_T t\arctan(2\omega_T t)+\frac{1}{2}\ln\left(\frac{1+\omega_c^2t^2}{1+4\omega_T^2t^2}\right)\right], \qquad (20)$$

where $c_1\equiv\alpha_1/\hbar^2$. On the other hand, an exact solution for the super-Ohmic case $d=3$ [Eq. (19)] can be found for any temperature T. The result is

$$\Gamma_3(t,T)=c_3\left\{\theta^2[\zeta(2,\theta)+\zeta(2,1+\theta)-\zeta(2,\theta+i\omega_T t) -\zeta(2,\theta-i\omega_T t)]+\frac{1-\omega_c^2t^2}{[1+\omega_c^2t^2]^2}\right\}, \qquad (21)$$

where $\zeta(z,q)=[1/\Gamma(z)]\int_o^\infty dt[t^{z-1}e^{-qt}/(1-e^{-t})]$ is the generalized Riemann zeta function, $\Gamma(z)=\int_o^\infty dt\,t^{z-1}e^{-t}$ is the Gamma function, and $c_3=\alpha_3\omega_c^2/\hbar^2$.

For the purpose of this paper, we concentrate on the case $L>1$ for which we have several results. We leave the analysis of the $L=1$ case to Appendix A, where we discuss the process of identifying typical decoherence times for a single qubit, and the interplay between the different decoherence regimes as a function of the temperature.

B. $L=2$ qubit register

Let us analyze the case of two qubits in the presence of the bosonic reservoir discussed in the present paper. Using the same expressions for the density of states $G(\omega)$ and for the frequency-dependent coupling $g(\omega)$ as above, we will analyze the coherence decay for several different input states. We set the qubits at positions r_a and r_b with coupling factors given by $g^n_{\mathbf{k}}=g_{\mathbf{k}}e^{-i\mathbf{k}\cdot\mathbf{r}_n}$, and $n=a,b$. It is easy to see that the unitary evolution operator induces entanglement between qubit states and field states: $U_I(t)$ acts as a conditional

displacement operator for the field with a displacement amplitude depending on both qubits of the QR, as discussed in more detail in [20]. As we have pointed out previously, it is this entanglement that is responsible for the decoherence processes described in the present paper. In particular, the case of two qubits has

$$\rho^{Q}_{i_a j_a, i_b j_b}(t) = \langle i_a, i_b | \mathrm{Tr}_B\{\rho^S(t)\} | j_a, j_b \rangle .$$

Next we analyze the register dynamics for the limiting decoherence situations described above. First, let us study the case of *independent decoherence*.

(i) $i_a = j_a, i_b \neq j_b$:

$$\rho^{Q}_{i_a i_a, i_b j_b}(t) = \exp[\, i\Theta_d(t) f_{i_a i_a, i_b j_b} - \Gamma_d(t;T)] \times \rho^{Q}_{i_a i_a, i_b j_b}(0),$$

where

$$f_{i_a i_a, i_b j_b} = 2 i_a (i_b - j_b) \cos \mathbf{k} \cdot \mathbf{r}_{ab} .$$

Hence, $f_{00,01} = f_{11,10} = \cos \mathbf{k} \cdot \mathbf{r}_{ab}$, and $f_{00,10} = f_{11,01} = -\cos \mathbf{k} \cdot \mathbf{r}_{ab}$: $\rho^{Q}_{i_a i_a, i_b j_b}(t)$ shows collective decay. This result is contrary to the one reported in Ref. [20].

(ii) $i_a = j_a$, $i_b = j_b$:

$$\rho^{Q}_{i_a i_a, i_b i_b}(t) = \rho^{Q}_{i_a i_a, i_b i_b}(0);$$

as expected, the populations remain unaffected.

(iii) $i_a \neq j_a, i_b \neq j_b$:

$$\rho^{Q}_{i_a j_a, i_b j_b}(t) = \exp[-\Gamma_d(t;T) h_{i_a j_a, i_b j_b}] \rho^{Q}_{i_a j_a, i_b j_b}(0),$$

where $h_{i_a j_a, i_b j_b} = 2[1 + (i_a - j_a)(i_b - j_b) \cos \mathbf{k} \cdot \mathbf{r}_{ab}]$. Clearly, $h_{10,10} = h_{01,01} = 2[1 + \cos \mathbf{k} \cdot \mathbf{r}_{ab}]$, and $h_{10,01} = h_{01,10} = 2[1 - \cos \mathbf{k} \cdot \mathbf{r}_{ab}]$. Hence, $\rho^{Q}_{i_a j_a, i_b j_b}(t)$ also shows collective decay.

In the above cases, analytic expressions for the corresponding decoherence functions can be found. As in Sec. III A, we shall consider two different surrounding environments. In the low-TE regime, the "Ohmic environment" ($d=1$) induces the following coherence decay (the high-TE requires numerical integration):

$$\rho^{\pm}_{d=1}(t) \approx \exp\left[-\Gamma_1(t,T) \pm i c_1 \left(\frac{1}{2} \arctan(\omega_c t_-) - \frac{1}{2} \arctan(\omega_c t_+) + \frac{\omega_c t}{1 + \omega_c^2 t_s^2} \right) \right] \rho^{\pm}_{d=1}(0) \quad (22)$$

for $i_a = j_a$, and $i_b \neq j_b$. For brevity, we have dropped the subindices of the reduced density matrix, and set $t_+ = t_s + t$, and $t_- = t_s - t$. For $i_a \neq j_a$, and $i_b \neq j_b$ we obtain the result

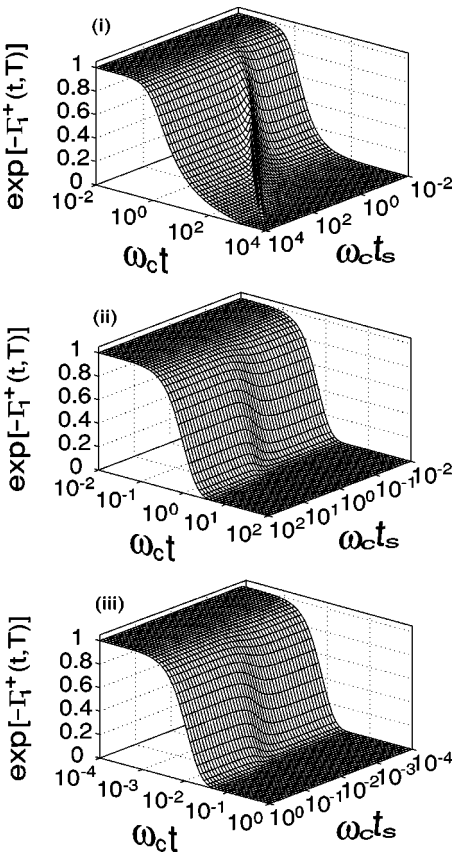

FIG. 1. Two-qubit "independent decoherence" due to the coupling to a reservoir of the Ohmic type ($d=1$) as a function of time t and the transit time t_s, for the input states associated with $\Gamma_1^+(t,T)(i_a \neq j_a, i_b \neq j_b)$. Here, $c_1 = 0.25$, and (i) $\theta = 10^{-3}$, (ii) 10^0, and (iii) 10^2. $\Gamma_i^{\pm}(t,T)$, with $i = 1,3$ are defined in the text.

$$\rho^{\pm}_{d=1}(t) \approx \exp\left[-2\Gamma_1(t,T) \mp 2c_1 \left(\frac{1}{4} \left\{ 2 \ln\left(\frac{1 + 4\omega_T^2 t_s^2}{1 + \omega_c^2 t_s^2} \right) + \ln\left(\frac{1 + \omega_c^2 t_-^2}{1 + 4\omega_T^2 t_-^2} \right) + \ln\left(\frac{1 + \omega_c^2 t_+^2}{1 + 4\omega_T^2 t_+^2} \right) \right\} - \omega_T \{ 2t_s \arctan(2\omega_T t_s) - t_- \arctan(2\omega_T t_-) - t_+ \arctan(2\omega_T t_+) \} \right) \right] \rho^{\pm}_{d=1}(0). \quad (23)$$

In Figs. 1 and 2, we have plotted the decay of two-qubit coherence due to the coupling to an environment of the Ohmic type [Eqs. (23)]. Here, $\Gamma_1^{\pm}(t,T)$ are defined from Eqs. (23) as $\rho^{\pm}_{d=1}(t) = \exp[-\Gamma_1^{\pm}(t,T)] \rho^{+}_{d=1}(0)$. From these figures we can see the variations of the onset of decay when increasing the temperature. Figure 1 shows how the departure of coherence from unity changes with t_s [plot 1 (i)], while for high temperature [plot 1 (iii)], there is no variation with t_s at all. In the limit of large t_s (see Table I), we recover the onset of decay of Fig. 6 (Appendix A). Note the difference between the time scales of plots 1 (i) and (iii), and how an estimation of typical decoherence times strongly relies on the

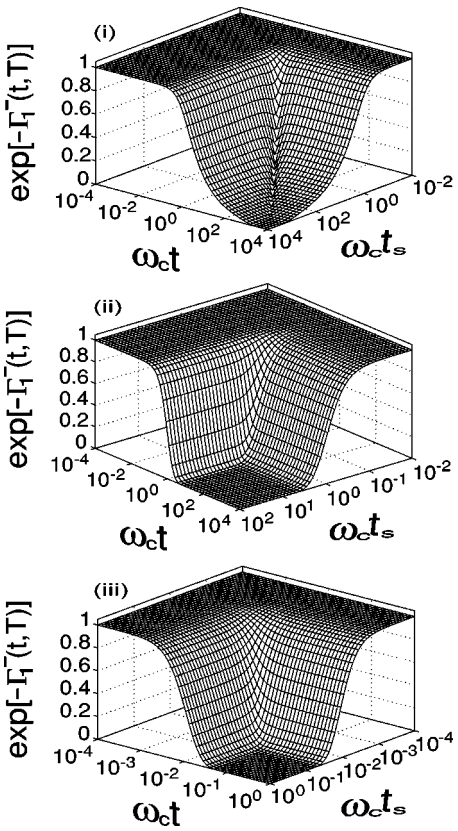

FIG. 2. Two-qubit "independent decoherence" caused by the coupling to an "Ohmic environment" as a function of times t and t_s, for the input states associated with $\Gamma_1^-(t,T)$ $(i_a \neq j_a, i_b \neq j_b)$. $c_1=0.25$, and (i) $\theta=10^{-3}$, (ii) 10^0, and (iii) 10^2.

temperature of the environment. Figure 2 shows how the coherence decay shown in Fig. 1 disappears for small t_s values, i.e., for a given temperature, it is possible to find a t_s from which there is no decoherence of the two-qubit system. This interesting behavior occurs only for the density-matrix elements $\langle 10|\mathrm{Tr}_B\{\rho^S(t)\}|01\rangle = \langle 01|\mathrm{Tr}_B\{\rho^S(t)\}|10\rangle$.

In Table I we give some typical two-qubit decoherence times τ_{dec} for an Ohmic environment in terms of the temperature, coupling constants c_1, and t_s. In all of the tables in this paper, we have taken the beginning of the decoherence process to occur when the reduced density matrix of the whole system exhibits a 2% deviation from the initial condition, i.e., when $\exp[-\Gamma_i(t\equiv\tau_{dec},T)]=0.98$. The tables have been generated from the corresponding decoherence functions reported in this paper. Here, t_f is defined from $\exp[-\Gamma_i(t=t_f,T)]=0.01$, i.e., the difference between t_f and τ_{dec} gives an estimate for the duration of the decoherence process, say t_{decay}; and $\tau_{dec}^{\pm}$, and $t_f^{\pm}$ are evaluated from the respective decoherence functions $\Gamma_i^{\pm}(t,T)$, with $i=1,3$. In order to gain insight into some characteristic time scales, consider, for example, the case of the solid state, where in many situations the noise field can be identified with the phonon field. Here the cutoff ω_c can be immediately associated with the Debye frequency ω_D. A typical Debye temperature $\Theta_D=100$ K has $\omega_D \equiv \omega_c \approx 10^{13}$ s^{-1}, so $\theta \equiv \omega_T/\omega_c \approx 10^{-2}T$. Hence we can see from Table I (Figs. 1 and 2) that for $c_1=0.25$, $\omega_c t_s=0.5$, and $T=0.1$ K, the decoherence process starts at $\tau_{dec}^+ \approx 23.5$ fs and $\tau_{dec}^- \approx 43.7$ fs, and it lasts for $t_{decay}^+ \approx 10.3$ ps (for t_{decay}^-, $\exp[-\Gamma_1^-(t\mapsto\infty,0.1\text{ K})]$ saturates above 0.01). If the strength of the coupling goes down to $c_1=0.01$, then $\tau_{dec}^+ \approx 0.2$ ps, and $t_{decay}^+ \approx 3.5$ ns. In this latter case, τ_{dec}^-, and

TABLE I. Characteristic times for two-qubit independent decoherence $\tau_{dec}^{\pm}$ for $(d=1)$-dimensional density of states of the field. Different temperature, transit time, and coupling strength values are considered. $i_a \neq j_a, i_b \neq j_b$ (see text).

c_1	$k_BT/\hbar\omega_c$	$\omega_c t_s$	$\omega_c\tau_{dec}^-$	$\omega_c t_f^-$	$\omega_c\tau_{dec}^+$	$\omega_c t_f^+$
0.25	10^{-3}	0.5	0.436919	saturates	0.235446	103.507
0.25	10^{0}	0.5	0.183755	saturates	0.104119	2.05958
0.25	10^{-3}	10^4	0.290113	1279.63	0.290113	1279.64
0.25	10^{0}	10^4	0.127778	3.459 01	0.127778	3.45901
0.1	10^{-3}	0.5	0.913573	saturates	0.37654	2025.75
0.1	10^{0}	0.5	0.303135	saturates	0.16504	4.28334
0.1	10^{-3}	10^4	0.47316	5669.66	0.473159	5670.15
0.1	10^{0}	10^4	0.203549	7.865 96	0.203549	7.86596
0.01	10^{-3}	0.5	saturates	saturates	1.45274	35004.7
0.01	10^{0}	0.5	saturates	saturates	0.538502	37.2732
0.01	10^{-3}	10^4	2.55738	saturates	2.55738	40816.8
0.01	10^{0}	10^4	0.709492	73.8325	0.709492	73.8325

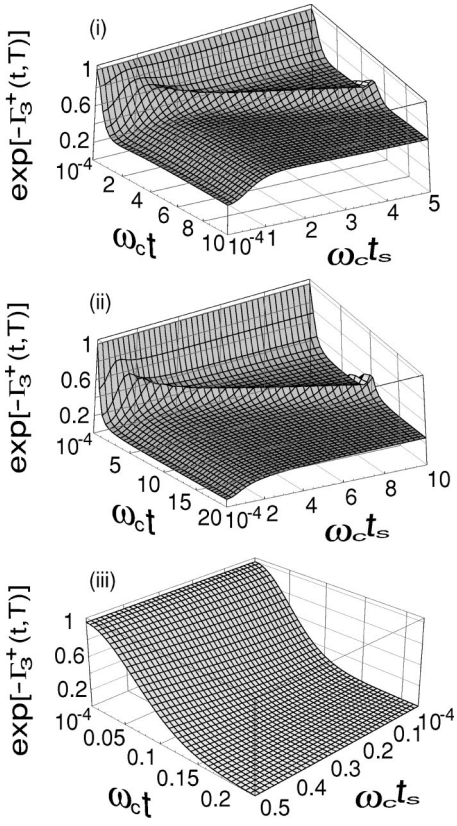

FIG. 3. Two-qubit "independent decoherence" due to the super-Ohmic environment $d=3$ [Eq. (25)] as a function of times t and t_s, for the input states associated with $\Gamma_3^+(t,T)$. $c_3=0.25$, and (i) $\theta=10^{-3}$, (ii) 10^0, and (iii) 10^2.

t^{-}_{decay} are not reported, since the coherence saturates to a value above 0.98. From the data reported in Table I, it is clear that the weaker the coupling between the qubits and the environment, the longer the decoherence times and the slower the decoherence process. In addition, the higher the temperature, the faster the qubits decohere, as expected intuitively.

The effect of the transit time becomes more evident from Table I: for large t_s values, there is no difference between τ^{+}_{dec} and τ^{-}_{dec} (also, $t^{+}_{decay} \approx t^{-}_{decay}$). This is because for large t_s, the contribution due to terms involving t_s in Eq. (23) is negligible, hence the reduced density-matrix $\rho^{\pm}_{\bar{d}=1}(t) \equiv \rho_{d=1}(t) \approx \exp[-2\Gamma_1(t,T)]$ and hence has a similar behavior to the single-qubit case [Eq. (19)]. Hence for large t_s (e.g., $t_s = 10^4$), Figs. 1 and 2 resemble the onset of decay of the single-qubit case (see later Fig. 6) where there is no dependence on t_s. We note that $\exp[-\Gamma^{+}_1(t,T)](\exp[-\Gamma^{-}_1(t,T)])$ is the corresponding decay of the coherences $\rho_{10,10} = \rho_{01,01}$ $(\rho_{10,01} = \rho_{01,10})$, hence, $\rho^{Q}_{10,10}(t) = \rho^{Q}_{10,01}(t)$ for large t_s.

By contrast, the super-Ohmic $d=3$ field leads to the following coherence decay:

$$\rho^{\pm}_{\bar{d}=3}(t) = \exp\Bigg[-\Gamma_3(t,T) \pm ic_3 \Bigg(\frac{\sin[2\arctan(\omega_c t_-)]}{2(1+\omega_c^2 t_-^2)} - \frac{\sin[2\arctan(\omega_c t_+)]}{2(1+\omega_c^2 t_+^2)} + \frac{2\omega_c t \cos[3\arctan(\omega_c t_s)]}{(1+\omega_c^2 t_s^2)^{3/2}} \Bigg) \Bigg] \rho^{\pm}_{\bar{d}=3}(0) \qquad (24)$$

for $i_a = j_a$, and $i_b \neq j_b$, and

$$\rho^{\pm}_{\bar{d}=3}(t) = \exp\Bigg[-2\Gamma_3(t,T) \mp 2c_3 \Bigg(-\frac{1-\omega_c^2 t_s^2}{[1+\omega_c^2 t_s^2]^2} + \frac{1-\omega_c^2 t_+^2}{2[1+\omega_c^2 t_+^2]^2} + \frac{1-\omega_c^2 t_-^2}{2[1+\omega_c^2 t_-^2]^2} + \frac{\theta^2}{2}\{2\zeta(2,\theta - i\omega_T t_s) + 2\zeta(2,\theta + i\omega_T t_s) - \zeta(2,\theta + i\omega_T t_+) - \zeta(2,\theta - i\omega_T t_+) - \zeta(2,\theta + i\omega_T t_-) - \zeta(2,\theta - i\omega_T t_-)\} \Bigg) \Bigg] \rho^{\pm}_{\bar{d}=3}(0) \qquad (25)$$

for $i_a \neq j_a$, and $i_b \neq j_b$. The results of Eqs. (24) and (25) are exact: no approximations have been made in obtaining them. Therefore, they are valid for any temperature of the environment.

In Figs. 3 and 4, we have plotted the decay of two-qubit coherence due to the coupling to a reservoir with three-dimensional density of states [Eqs. (25)]. Some estimates for τ_c and t_{decay} have been given in Table II. The decoherence functions $\Gamma^{\pm}_3(t,T)$ are defined as $\rho^{\pm}_{\bar{d}=3}(t) = \exp[-\Gamma^{\pm}_3(t,T)]\rho^{\pm}_{\bar{d}=3}(0)$. As we can see, there is a *nonmonotonic* behavior for the decay of coherence for low-temperature values, as can be seen from Figs. 3(i), and 3(ii). The decay given by the functions $\Gamma^{+}_3(t,T)$ (Fig. 3) and $\Gamma^{-}_3(t,T)$ (Fig. 4) saturates to a particular value, which is fixed by the strength of the coupling and the temperature of the reservoir: the lower the temperature, the slower the decay, and the higher the residual coherence. Some estimates for these saturation values $e^{-\Gamma^{\pm}_3(t^{\pm}_f,T)}$ are shown in Table II. From Fig. 4, it is possible to find small t_s values for which the onset of decay does not change in time and coherence remains unaffected. This result is very different from the case of Fig. 3, where coherence either vanishes (at high temperatures) or saturates to a residual coherence value (at low temperatures). Also, note that while nothing happens to the onset of decay of Fig. 4, the coherence decay is amplified in the case of Fig. 3, for small t_s values. From Figs. 3(i) and 3(ii) and Figs. 4(i) and 4(ii), we see that there is saturation of the decay in the presence of a *nontrivial* coherence process. However, for high temperatures [Figs. 3(iii) and 4(iii)] there is a monotonic behavior where no saturation occurs at all and the residual coherence vanishes. We note that the nonmonotonic behavior reported here for the low-temperature regime is not just a characteristic of high-dimensionality fields: it also occurs for the $d=1$ field, as can be seen from Figs. 1(i)

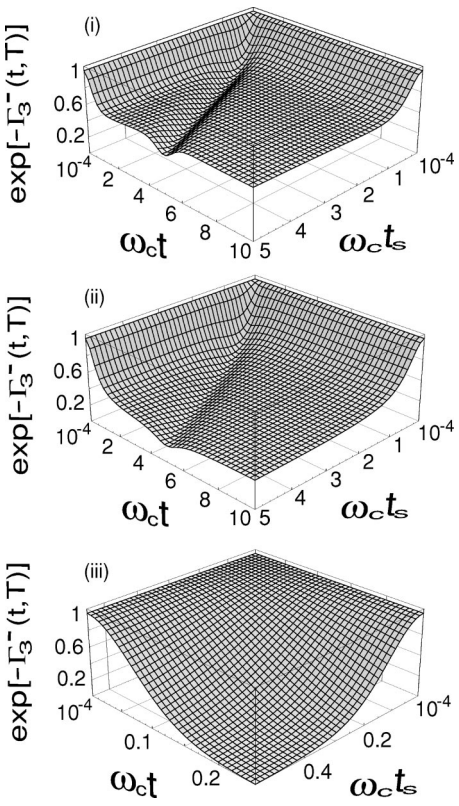

FIG. 4. Two-qubit ''independent decoherence'' due to the super-Ohmic environment $d=3$ as a function of times t and t_s for the input states associated with $\Gamma^{-}_3(t,T)$. $c_3 = 0.25$, and (i) $\theta = 10^{-3}$, (ii) 10^0, and (iii) 10^2.

TABLE II. Characteristic times for two-qubit independent decoherence $\tau_{dec}^{\pm}$ for $(d=3)$-dimensional density of states of field. $i_a \neq j_a, i_b \neq j_b$.

c_3	ω_T/ω_c	$\omega_c t_s$	$\omega_c \tau_{dec}^{+}$	$\omega_c t_f^{+}$	$e^{-\Gamma_3^{+}(t_f^{+})}$	$\omega_c \tau_{dec}^{-}$	$\omega_c t_f^{-}$	$e^{-\Gamma_3^{-}(t_f^{-})}$
0.25	10^{-3}	0.5	0.1292	sat.	0.477	0.10818	sat.	0.771
0.25	10^{2}	0.5	0.01338	0.20	0.01	0.01522	0.24	0.01
0.25	10^{-3}	10^{2}	0.11738	sat.	0.6065	0.11738	sat.	0.6065
0.25	10^{2}	10^{2}	0.01421	0.22	0.01	0.01421	0.22	0.01
0.01	10^{-3}	0.5	0.79957	sat.	0.971	sat.	sat.	0.989
0.01	10^{2}	0.5	0.066994	1.51	0.01	0.07645	sat.	0.449
0.01	10^{-3}	10^{2}	9.7767	sat.	0.9802	9.7767	sat.	0.9802
0.01	10^{2}	10^{2}	0.07124	sat.	0.01831	0.07124	sat.	0.01832

and 2(i). We believe that this purely quantum-mechanical phenomenon is associated with an interplay between the quantum vacuum and thermal fluctuations of the system and the quantum character of the field. The system undergoes dynamics where the environment manages to ''hit back'' at the qubits in such a way that the coherences then exhibit an effective revival before vanishing (at high temperatures) or saturating to a residual value (at low temperatures). An essential feature of the model studied here is the fact that the QR and bath are assumed to be initially uncorrelated. In future work, we will analyze the behavior of these ''recoherences'' with more general initial conditions, where the initial state of the combined system is allowed to contain some correlations between the bath and the QR (see also Ref. [28]). Such studies will help to clarify the origins of this ''recoherence effect'' and also the effectiveness of decoherence as a function of the initial conditions. We note that there is a previous work by Hu *et al.* [30] where the study of quantum Brownian motion in a general environment gives rise to a similar behavior (although in a different context) to the one reported here for the ''recoherences.'' A more detailed analysis of the physical implications of this interesting behavior of the coherence decay is intended to be addressed elsewhere [31].

It is interesting that the dynamics of coherences depend so strongly on the strength of the coupling. It can be seen from Table II and Fig. 5 that (i) the coherences saturate (sat.) to a very high ''residual value'' and show less than a 2% decay for weak coupling (e.g., $c_3=0.01$) and low temperatures ($T=0.1$ K). This result is to be compared with the $d=1$ case where the coherences always vanish for long t_s; (ii) even at high temperatures ($T=10^4$ K), where the coherences vanish, and weak coupling, we find the appearance of the ''recoherence effect'' discussed above. This makes more evident the role of the QR-bath coupling: recoherences should appear only under certain conditions imposed by the strength c_3 (hence by the spectral density) and the temperature. These conditions can be directly obtained from the decoherence functions reported in this paper. Typical $\tau_{dec}^{\pm}$ times for this $(d=3)$-dimensional environment are given in Table II. From these we can conclude that the two QR decoherence time scales are shorter, and the decoherence process occurs faster, than in the single-qubit case.

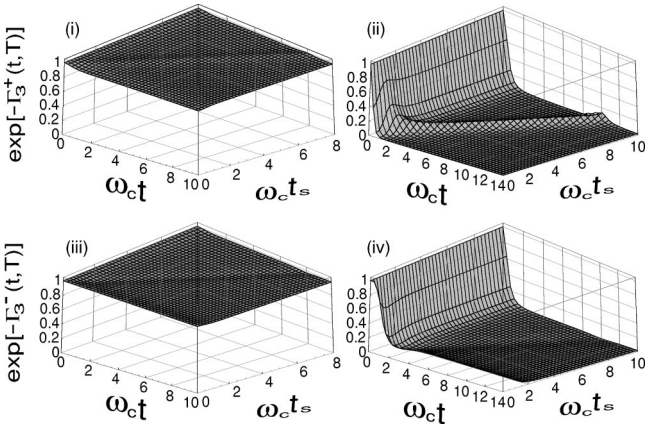

FIG. 5. Two-qubit ''independent decoherence.'' $d=3$, coupling strength $c_3=0.01$, and (i),(iii) $\theta=10^{-3}$, and (ii),(iv) $\theta=10^{2}$.

We now analyze how the above results are affected when we consider the situation of *collective decoherence*, as given by Eq. (16). The reduced density matrix for the two qubit system now reads $\rho^{Q}_{i_a j_a, i_b j_b}(t)=\exp\{i\Theta_d(t)[(\Sigma_{m=a}^{b} i_m)^2 - (\Sigma_{m=a}^{b} j_m)^2]\}\exp\{-\Gamma_d(t;T)[\Sigma_{m=a}^{b}(i_m-j_m)]^2\}\rho^{Q}_{i_a j_a, i_b j_b}(0)$. In particular, we find

(i) $i_a=j_a, i_b\neq j_b$: $\rho^{Q}_{i_a i_a, i_b j_b}(t)=\exp[i\Theta_d(t) f'_{i_a i_a, i_b j_b} - \Gamma_d(t;T)]\rho^{Q}_{i_a i_a, i_b j_b}(0)$, where $f'_{i_a i_a, i_b j_b}=2i_a(i_b-j_b)$. Hence $f'_{00,01}=f'_{11,10}=1$, and $f'_{00,10}=f'_{11,01}=-1$. The corresponding decoherence rates are

$$\rho^{\pm}_{d=1}(t)\approx\exp\{-\Gamma_1(t,T)\pm ic_1[\omega_c t+\arctan(\omega_c t)]\}\rho^{\pm}_{d=1}(0),$$

$$\rho^{\pm}_{d=3}(t)=\exp\left[-\Gamma_3(t,T)\pm ic_3 \times\left(2\omega_c t-\frac{\sin[2\arctan(\omega_c t)]}{1+\omega_c^2 t^2}\right)\right]\rho^{\pm}_{d=3}(0) \tag{26}$$

for the Ohmic environment and the $(d=3)$-dimensional density of states, respectively.

(ii) $i_a=j_a, i_b=j_b$: $\rho^{Q}_{i_a i_a, i_b i_b}(t)=\rho^{Q}_{i_a i_a, i_b i_b}(0)$: as expected, the populations remain unaffected.

(iii) $i_a\neq j_a, i_b\neq j_b$:

$$\rho^{Q}_{i_a j_a, i_b j_b}(t) = \exp[-\Gamma_d(t;T) h'_{i_a j_a, i_b j_b}] \rho^{Q}_{i_a j_a, i_b j_b}(0),$$

where $h'_{i_a j_a, i_b j_b} = (i_a + i_b - j_a - j_b)^2$. Then, $h'_{10,10} = h'_{01,01} = 4$, and $h'_{10,01} = h'_{01,10} = 0$. Obviously, the corresponding decoherence rates are

$$\rho^{-}_{d=1}(t) = \rho^{-}_{d=1}(0),$$

$$\rho^{+}_{d=1}(t) \approx \exp[-4\Gamma_1(t,T)] \rho^{+}_{d=1}(0) \tag{27}$$

for the $(d=1)$-dimensional field, and

$$\rho^{-}_{d=3}(t) = \rho^{-}_{d=3}(0),$$

$$\rho^{+}_{d=3}(t) \approx \exp[-4\Gamma_3(t,T)] \rho^{+}_{d=3}(0) \tag{28}$$

for the $(d=3)$-dimensional field. Hence, regarding the input states, the case of *collective decoherence* shows two very well defined situations.

(a) A set of input states that shows no decoherence at all, despite the fact that the qubits are interacting with the environment. This is because under the specific situation of collective coupling there is a set of initial qubit states that does not entangle with the bosonic field and hence the states preserve their coherence. These states are the so-called ''coherence-preserving'' states and, for the case of a 2-QR, the corresponding reduced density-matrix elements are $\langle 10|\mathrm{Tr}_B\{\rho^S(t)\}|01\rangle$, and $\langle 01|\mathrm{Tr}_B\{\rho^S(t)\}|10\rangle$. As studied in more detail in Ref. [13] (where relaxation effects are also included), this result can be used as an encoding strategy, where an arbitrary L-QR can be decoupled from its environment provided that every single qubit of the register can be encoded using two qubits: e.g., using the simple encoding (though not the most efficient one) $|0\rangle \mapsto |01\rangle$, and $|1\rangle \mapsto |10\rangle$. It turns out that this procedure is ensured even if relaxation effects are included in the Hamiltonian (1) [13]. Hence in the specific situation of collective decoherence one can find, for arbitrary L, a decoherence-free subspace (DFS) $C_L \in \mathcal{H}^{\otimes L}$ (the Hilbert space $\mathcal{H} = \mathcal{H}_{QR} \otimes \mathcal{H}_B$) that does not get entangled with the environment, and hence, the QR should evolve without decoherence. Besides quantum error correction codes, this is currently one of the most outstanding results in the battle against decoherence [13], particularly because of its relevance to maintaining a coherent qubit memory in quantum information processing.

(b) The other two input states have the decay of coherences $\langle 11|\mathrm{Tr}_B\{\rho^S(t)\}|00\rangle$ and $\langle 00|\mathrm{Tr}_B\{\rho^S(t)\}|11\rangle$: these give a situation of ''superdecoherence'' [20], where the qubits are collectively entangled, and hence, these matrix elements give the fastest decay for the coherences. This means that while there is a subspace which is robust against decoherence as discussed above, the remaining part of the Hilbert space gets strongly entangled with the environment. This superdecoherence situation is illustrated in Fig. 6 for the case of reservoirs with one- and three-dimensional density of states. The above process of calculating explicit results for the decay of any coherence associated with the coupling of a L-QR to a bosonic reservoir, for both types of coupling (independent and collective), can be carried out for any $L > 2$ using the general formulas Eqs. (12) and (16). In so doing, we can obtain an estimate of typical decoherence times for a QR with an arbitrary number of qubits. We should point out that if no schemes for controlling the errors induced by the decoherence phenomenon are used [11–17], τ_{dec} establishes an upper bound to the duration of any reliable quantum computing process.

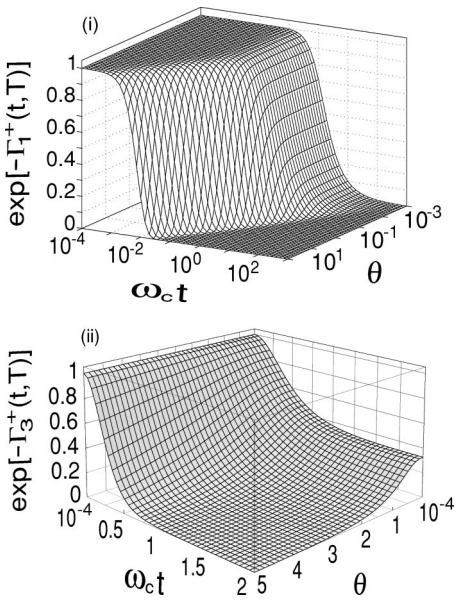

FIG. 6. Two-qubit ''collective decoherence'' for (i) $d=1$ ''Ohmic environment'' [Eq. (27)], and (ii) $d=3$ ''super-Ohmic environment'' [Eq. (28)], as a function of time and the temperature $\theta \equiv \omega_T/\omega_c$. $c_1 = c_3 = 0.25$, and $i_a \neq j_a$, and $i_b \neq j_b$. $\Gamma^{+}_{d}(t,T)(d=1,3)$ is defined using Eqs. (27) and (28).

IV. DISCUSSIONS AND CONCLUDING REMARKS

We have revisited a model of decoherence based upon the one previously studied by Leggett *et al.* [22] in connection with the tunneling problem in the presence of dissipation, and used later by Unruh [32] and Palma *et al.* [20] for describing the decoherence process of a quantum register. We have presented here a more complete description of this latter problem, which provides the following results. The decoherence rates of the density-matrix elements are correctly derived, leading to quantitative results for both independent and collective decoherence situations. As discussed here, if no error correcting/preventing strategies are used, this has implications for an estimation of decoherence time scales for which the quantum memory of a QR can be maintained in any reliable computation (we note, however, there has been a recent proposal by Beige *et al.* regarding the use of dissipation to remain and manipulate states within a DFS [14]). Our results agree with those reported in [21] for the case of collective decoherence but they are different to the ones reported there for the case of independent decoherence: in Ref. [21], it is argued that independent decoherence, as opposed to collective decoherence, is insensitive to the qubit input states. Here, we have shown instead that both cases are very sensitive to the input states and that both of them show collective decay.

In the specific situation of independent decoherence we have found a nontrivial behavior in the decay of the off-diagonal elements of the reduced density matrix. Here, the coherences experience an effective revival before they either vanish or saturate to a residual value. This behavior depends on the temperature of the environment and depends strongly on the strength of the coupling: the coherence dynamics are different in the weak and strong coupling regime. Also, there are important qualitative differences between the Ohmic $d=1$ and the super-Ohmic environment $d=3$, which is ultimately linked to the spectral density of the bath. In the former case the coherence is always lost, while in the latter the coherence generally saturates to a residual value which is fixed by the temperature and strength of the coupling and *only* vanishes in the high-TE. By contrast, in the case of collective decoherence, we have identified QR input states that allow the system to evolve in a decoherence-free fashion, the so-called coherence-preserving states. We note that DFS's do not exist in the specific situation of independent qubit decoherence. We also note that our attention has been drawn to a dynamical-algebraic description that unifies the currently known quantum errors stabilization procedures [27] (see also Refs. [16,26]). Within the framework of a system formed by a collection of L uncorrelated clusters of subsystems where each cluster fulfills the requirements of collective decoherence, Zanardi has shown that noiseless subsystems can be built [27].

From the point of view of complexity analysis (and without including any strategy for the stabilizing of quantum information), we should ask how the results reported in the present paper affect those of Ref. [20]. We must identify the coherences that are destroyed more rapidly: from Eqs. (12) and (16) it is easy to see that the coherences with the fastest decay are given by the matrix elements $\rho_{\{0_n,1_n\}}$ and $\rho_{\{1_n,0_n\}}$. These off-diagonal elements decay as $\exp[-\Gamma_d(t;T)f(L)]$, with

$$f(L)=L+2\sum_{\substack{m=1,n=2\\ m\neq n}}^{L}(i_m-j_m)(i_n-j_n)\cos(\omega t_s), \quad (29)$$

for the limit of independent qubit decoherence, and as $\exp[-L^2\Gamma_d(t;T)]$ for the collective decoherence case. Hence, it is clear that for both cases, the longer the QR coherence length, the faster the coherence decay. Despite the fact that the results of Palma *et al.* [20] are not the same as ours, it turns out that both sets of results lead to the same unwelcome exponential increase of the error rate. We note that the result of Eq. (29) is in general different from the one reported in [20]. We also note that the coherence decay for the case of collective decoherence coincides with that of [20] only for the fastest off-diagonal element decay: if we consider different density-matrix elements, the results of Ref. [20] no longer coincide with ours. If the information reported in our paper is used for an estimation of the actual decoherence time associated with any given off-diagonal density-matrix element (coherence), the results are in general quite different from the ones reported in [20].

We have shown how a bosonic environment destroys the coherences of an arbitrary quantum register. In doing so, we have identified DFS states that are invariant under the coupling to such an environment. This result could be of crucial importance for improving the efficiency of quantum algorithms, for example. We believe that the engineering of DFS's will become intrinsic to the designs of future quantum computation architectures. There was a recent experimental demonstration of decoherence-free quantum memories [18,19]. This has been achieved for *one* qubit, by encoding it into the DFS of a pair of trapped $^9Be^+$ ions: in this way, Kielpinski *et al.* have demonstrated the immunity of a DFS of two atoms to collective dephasing [18]. Prior to this experiment with trapped ions, Kwiat *et al.* demonstrated the robustness of a DFS for two photons to collective noise [19]. Robust quantum memories seem therefore to be well on their way, both theoretically and experimentally, to overcoming the main obstacle to quantum information processing—namely, decoherence.

ACKNOWLEDGMENTS

We are grateful to L. Viola for a critical reading of the manuscript. J.H.R. acknowledges H. Steers for continuous encouragement and G. Hechenblaikner for stimulating discussions. J.H.R. is grateful for financial suppport from the Colombian Government Agency for Science and Technology (COLCIENCIAS). L.Q. was partially supported by COLCIENCIAS under Contract No. 1204-05-10326. N.F.J. thanks EPSRC for support.

APPENDIX A: SINGLE-QUBIT DECOHERENCE

The decoherence rates for a single qubit coupled to a reservoir with $d=1$, and $d=3$ density of states are [Eq. (19)]

$$\Gamma_1(t,T)=\frac{\alpha_1}{\hbar^2}\int d\omega e^{-\omega/\omega_c}\frac{1-\cos(\omega t)}{\omega}\coth\left(\frac{\omega}{2\omega_T}\right) \quad (A1)$$

$$\Gamma_3(t,T)=\frac{\alpha_3}{\hbar^2}\int d\omega\omega e^{-\omega/\omega_c}[1-\cos(\omega t)]\coth\left(\frac{\omega}{2\omega_T}\right). \quad (A2)$$

In Sec. III A, we gave the analytic solutions to these integrals. However, we did not perform a full analysis of those results. We start here by recalling that the solution found for the integral (A1) was an approximate one, valid only for the low-TE ($\omega_T\ll\omega_c$): a general solution to this integral requires numerical integration. The second integral was solved analytically for any temperature value T (without making any approximation). In these calculations, note that the constant coupling α_d changes its units with the dimensionality of the field: $[\alpha_1]=[(\mathrm{eV})^2\mathrm{s}^2]$, $[\alpha_3]=[(\mathrm{eV})^2\mathrm{s}^4]$, etc.

We first analyze the case $d=1$. In the low-TE, Eq. (20) leads to the identification of three main regimes for the decay of the coherences: (a) a ''quiet'' regime, for which $t<\tau_c$, and $\Gamma_1(t,T)\approx c_1\omega_c^2t^2/2$; (b) a ''quantum'' regime, where $\tau_c<t<\tau_T$, and $\Gamma_1(t,T)\approx c_1\ln(\omega_c t)$; and (c) a ''thermal'' re-

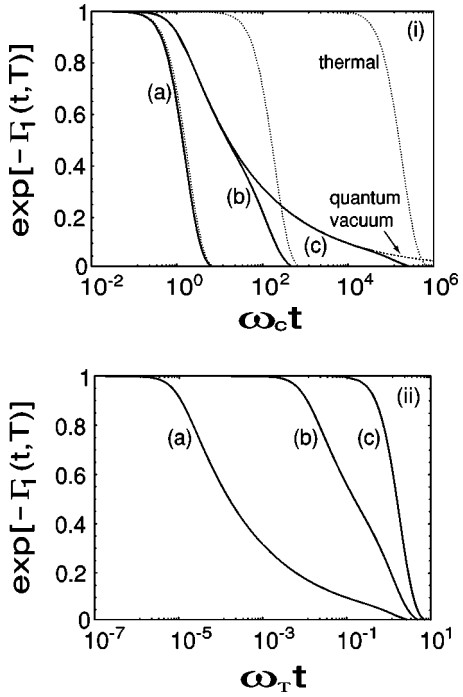

FIG. 7. (i) Decoherence of a single qubit for an "Ohmic environment" as a function of t (in units of ω_c). The contributions arising from the separate integration of thermal ($\exp[-\Gamma_T(t)]$) and vacuum ($\exp[-\Gamma_V(t)]$) fluctuations are shown as dotted curves. $c_1=0.25$, (a) $\theta\equiv\omega_T/\omega_c=1$, (b) 10^{-2}, (c) 10^{-5}. If ω_c is the Debye cutoff, $\theta\approx 10^{-2}T$ (see text): the decoherence shown corresponds to $T=100$ K, $T=1$ K, and $T=1$ mK, respectively. (ii) Coherence decay for (a) $\theta=10^{-5}$, (b) 10^{-2}, (c) 10^{2}. $c_1=0.25$. Here, time is given in units of the thermal frequency $\omega_T\equiv k_BT/\hbar$.

gime, for which $t\gg\tau_T$, and $\Gamma_1(t,T)\approx 2c_1\omega_T t$. These regimes have also been discussed in Refs. [20,32] and can be easily identified in Fig. 7 for several different temperatures. In Fig. 7(i) we have plotted Eq. (19) as a function of $\omega_c t$ for several different temperatures and for $d=1$. Since the decoherence effects arising from thermal noise can be separated from the ones due to quantum vacuum fluctuations, we have also plotted these partial contributions in order to see their effects over the time scales involved in the decoherence of the single qubit [Eq. (A1)]. It can be seen that for a given value of the temperature parameter θ, a characteristic time for which we start observing deviation of coherence from unity is determined by the shortest of the two time scales τ_c and τ_T, and that this value is increased when decreasing the temperature T, as expected. From Fig. 7(ic), it can clearly be seen that at low temperatures, the quantum vacuum fluctuations play the major role in eroding the qubit coherence, while the contribution due to thermal fluctuations plays a minor role. From this plot, we can see the three main regimes indicated above: a quiet ($t<\tau_c$), a quantum ($\tau_c<t<\tau_T$), and a thermal ($t>\tau_T$) regime. In this limit of low-TE, τ_c is the characteristic time that signals the departure of coherence from unity. Here, the qubit dynamics shows a competition between contributions arising from vacuum and thermal fluctuations: even at thermal time scales, the contribution to the decoherence due to vacuum fluctuations remains important.

TABLE III. Single-qubit decoherence times for different temperatures, and coupling strength $c_i(i=1,3)$; for $d=1$ (Ohmic), and $d=3$ (super-Ohmic) dimensional density of states of the field.

d	c_i	ω_T/ω_c	$\omega_c\tau_{dec}$	$e^{-\Gamma_i(\tau_{dec})}$	$\omega_c t_f$	$e^{-\Gamma_i(t_f)}$
	0.25	10^{-5}	0.418831	0.98	273950.34	0.01
	0.25	1.0	0.181611	0.98	6.39891	0.01
$d=1$	0.1	10^{-5}	0.705612	0.98	1153307.91	0.01
	0.1	1.0	0.291365	0.98	15.19703	0.01
	0.01	10^{-5}	7.47367	0.98	14346140.39	0.01
	0.01	1.0	1.09604	0.98	147.12606	0.01
	0.25	10^{-5}	0.167969	0.98	saturates	0.778801
	0.25	1.0	0.154762	0.98	saturates	0.564132
	0.25	10^{2}	0.020104	0.98	0.318417	0.01
$d=3$	0.1	10^{-5}	0.275766	0.98	saturates	0.904837
	0.1	1.0	0.251550	0.98	saturates	0.795339
	0.1	10^{2}	0.031791	0.98	0.546769	0.01
	0.01	10^{2}	0.101012	0.98	saturates	0.135331

In the case of the high-TE, the decay due to thermal noise [see dashed line in Fig. 7(ia)] becomes more important than the vacuum fluctuation contribution [33] and the start of the decoherence process is ruled by τ_T. Similar conclusions can be obtained from Fig. 7(ii), where the decay of coherence has been plotted as a function of time but in units of the thermal frequency ω_T for several different temperatures.

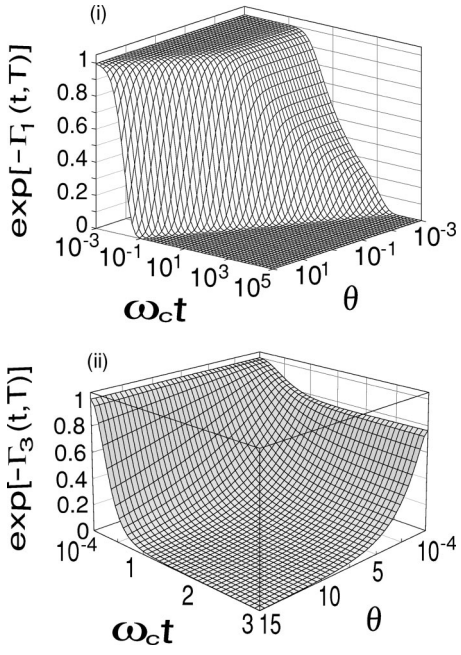

FIG. 8. Decoherence of a single qubit for (i) $d=1$, and (ii) $d=3$, as a function of time (in units of the cutoff ω_c) and the temperature parameter $\theta\equiv\omega_T/\omega_c$. $c_1=c_3=0.25$. If ω_c is the Debye cutoff, the range of coherence decay goes from a few mK up to (a) 10^4 K [plot (i)] and (b) 1.5×10^3 K [plot (ii)].

We can see from Table III and Fig. 7 that t_{decay} is comparable to τ_c for the high-TE, and to τ_T for the low-TE. Indeed, if we assume ω_c to be the Debye cutoff ($\omega_c \sim 10^{13}$ s^{-1}), we obtain from Table III that for $c_1=0.25$, and $T=1$ mK, the decoherence process starts at $\tau_{dec}\approx 41.9$ fs and lasts for $t_{decay}\approx 27.4$ ns (for $d=1$). Here, $\omega_T=1.3\times 10^{11}T\approx 1.3\times 10^{8}$ s^{-1}, hence $\tau_T\sim 8$ ns is of the same order of magnitude as t_{decay}. For the super-Ohmic environment $d=3$ (c_3 and T as before) we obtain $\tau_{dec}\approx 16.8$ fs. In this case, the coherences saturate to a residual value, as we discuss below [see Table III and Fig. 8(ii)]. From Table III, we can also see the effects of the high-TE: the qubit decoheres several orders of magnitude faster than in the low-TE case. For example, for $T=100$ K, $k_BT>\hbar\omega_c(\hbar\omega_c=6.58$ meV), and we obtain $\tau_{dec}\approx 18.1$ fs, and $t_{decay}\approx 0.6$ ps ($c_1=0.25,d=1$). A similar behavior is also observed in the $d=3$ case. In Table III we can appreciate the effect of the coupling strength on the decoherence time scales. Let $c_1=0.01$ ($d=1$), hence, for (i) $T=1$ mK, $\tau_{dec}\approx 0.75$ ps, and $t_{decay}\approx 1.4$ μs; for (ii) $T=100$ K, $\tau_{dec}\approx 0.11$ ps, and $t_{decay}\approx 14.6$ ps. Hence the weaker the coupling between the qubit and the environment, the longer the decoherence times and the slower the duration of the decoherence process. This result also holds for the case $d=3$, as can be seen from Table III. All of the above analysis concerning the different regimes for the decay of the coherences presented here is explicitly illustrated in the three-dimensional plots of Fig. 8.

Next, we analyze the decoherence behavior of the single qubit when coupling to the super-Ohmic $d=3$ reservoir. The corresponding decoherence function is given by Eq. (21). As can be seen from Fig. 8(ii) and Table III, this case shows an interesting behavior for the coherence decay: once the end of the ''quiet'' regime has been reached, the coherences decay to either zero, as in the case of Fig. 8(i), or saturate to a particular value determined by the temperature parameter ω_T/ω_c. Here we can identify the particular temperature value for which no saturation occurs at all and the expected decoherence takes place. In Table III, we give some saturation values for different temperatures and coupling strengths c_3. For $c_3=0.1$, and 0.25, the temperature value for which any residual coherence vanishes falls in the interval $10<\theta<100$ (high-TE). Apparently, these residual values shown in Fig. 8(ii) and Table III vanish when additional frequency modes associated with the three-dimensionality of the field are taken into account [20]. Even if this is not the case, surely the effects of relaxation mechanisms would mark the extent of these residual values.

APPENDIX B: TIME EVOLUTION AND THE REDUCED DENSITY MATRIX

In this appendix, we give details of the main steps followed in the calculation of the reduced density matrix given by Eq. (15).

1. The time evolution operator $U_I(t)$

Since Eq. (3) gives $H_I(t)=\Sigma_{n,\mathbf{k}}J_z^n(g_{\mathbf{k}}^n e^{i\omega_k t}b_{\mathbf{k}}^\dagger + g_{\mathbf{k}}^{*n}e^{-i\omega_k t}b_{\mathbf{k}})$, we have that

$$U_I(t)=T\exp\left[-\frac{i}{\hbar}\int_o^t\sum_{\mathbf{k}} g_{\mathbf{k}}(e^{i\omega_k t'}J_z^{\mathbf{k}}b_{\mathbf{k}}^\dagger+e^{-i\omega_k t'}J_z^{\dagger\mathbf{k}}b_{\mathbf{k}})dt'\right], \tag{B1}$$

where we have introduced the shorthand notation $J_z^{\mathbf{k}}=\Sigma_n e^{-i\mathbf{k}\cdot\mathbf{r}_n}J_z^n$. Hence, we can rewrite Eq. (B1) as [34]

$$\begin{aligned}U_I(t)=&\exp\left[\sum_{\mathbf{k}} g_{\mathbf{k}}\varphi_{\omega_k}(t)J_z^{\mathbf{k}}b_{\mathbf{k}}^\dagger\right]\\&\times T\exp\left[-\frac{i}{\hbar}\int_o^{t'}dt'\sum_{\mathbf{k}} e^{-i\omega_k t'}\right.\\&\times\exp\left(-\sum_{\mathbf{k}'} g_{\mathbf{k}'}\varphi_{\omega_{k'}}(t')J_z^{\mathbf{k}'}b_{\mathbf{k}'}^\dagger\right)g_{\mathbf{k}}J_z^{\dagger\mathbf{k}}b_{\mathbf{k}}\\&\left.\times\exp\left(\sum_{\mathbf{k}'} g_{\mathbf{k}'}\varphi_{\omega_{k'}}(t')J_z^{\mathbf{k}'}b_{\mathbf{k}'}^\dagger\right)\right].\end{aligned} \tag{B2}$$

It is easy to show that the calculation of the product given by the last two lines of Eq. (B2) gives the result

$$g_{\mathbf{k}}J_z^{\dagger\mathbf{k}}[b_{\mathbf{k}}+g_{\mathbf{k}}\varphi_{\omega_k}(t)J_z^{\mathbf{k}}]. \tag{B3}$$

Hence, the following expression for $U_I(t)$ arises:

$$\begin{aligned}U_I(t)=&\exp\left(\sum_{\mathbf{k}} g_{\mathbf{k}}\varphi_{\omega_k}(t)J_z^{\mathbf{k}}b_{\mathbf{k}}^\dagger\right)\exp\left(-\sum_{\mathbf{k}} g_{\mathbf{k}}\varphi_{\omega_k}^*(t)J_z^{\dagger\mathbf{k}}b_{\mathbf{k}}\right)\\&\times\exp\left\{-\frac{i}{\hbar}\sum_{\mathbf{k}}|g_{\mathbf{k}}J_z^{\mathbf{k}}|^2\int_o^t dt'\,\varphi_{\omega_k}(t')e^{-i\omega_k t'}\right\}\\=&\exp\left\{\sum_{\mathbf{k}} g_{\mathbf{k}}[\varphi_{\omega_k}(t)J_z^{\mathbf{k}}b_{\mathbf{k}}^\dagger-\varphi_{\omega_k}^*(t)J_z^{\dagger\mathbf{k}}b_{\mathbf{k}}]\right\}\\&\times\exp\left\{\sum_{\mathbf{k}}|g_{\mathbf{k}}J_z^{\mathbf{k}}|^2\left[\frac{it}{\hbar^2\omega_k}-\frac{\varphi_{\omega_k}^*(t)}{\hbar\omega_k}+\frac{|\varphi_{\omega_k}(t)|^2}{2}\right]\right\},\end{aligned} \tag{B4}$$

where we have used the result $e^{A+B}=e^Ae^Be^{-[A,B]/2}$, which holds for any pair of operators A,B that satisfy $[A,[A,B]]=0=[B,[A,B]]$ [as in the case of Eq. (B4)]. It is straightforward to see that Eq. (B4) gives the final result

$$\begin{aligned}U_I(t)=&\exp\left[i\sum_{\mathbf{k}}|g_{\mathbf{k}}|^2\frac{\omega_k t-\sin(\omega_k t)}{(\hbar\omega_k)^2}J_z^{\dagger\mathbf{k}}J_z^{\mathbf{k}}\right]\\&\times\exp\left[\sum_{\mathbf{k}}\{A_{\mathbf{k}}^\dagger(t)-A_{\mathbf{k}}(t)\}\right],\end{aligned} \tag{B5}$$

where $A_{\mathbf{k}}(t)=g_{\mathbf{k}}^*\varphi_{\omega_k}^*(t)J_z^{\dagger\mathbf{k}}b_{\mathbf{k}}$.

2. The reduced density matrix of a L-qubit register

We start by using the result for $U_I(t)$ in order to calculate the decay of the coherences, i.e., $\mathrm{Tr}_B[\rho^B(0)U_I^{\dagger\{j_n\}}(t)U_I^{\{i_n\}}(t)]$, with $U_I^{\{i_n\}}(t)$ as defined in Eq. (10). In so doing, we first compute the operator algebra for

the product $U_I^{\dagger\{j_n\}}(t)U_I^{\{i_n\}}(t)$ by taking into account the expression (B5). The result gives

$$U_I^{\dagger\{j_n\}}(t)U_I^{\{i_n\}}(t)=\exp\left[i\sum_{\mathbf{k}} |g_{\mathbf{k}}|^2\frac{\omega_k t-\sin(\omega_k t)}{(\hbar\omega_k)^2} \times\sum_{m,n}(i_m i_n-j_m j_n)\cos\mathbf{k}\cdot\mathbf{r}_{mn}\right] \times\exp\left[i\sum_{\mathbf{k}} |g_{\mathbf{k}}\varphi_{\omega_k}(t)|^2 \times\sum_{m,n} i_m j_n \sin\mathbf{k}\cdot\mathbf{r}_{mn}\right] \times\exp\left[\sum_{\mathbf{k}}(\sigma_{\mathbf{k}}b_{\mathbf{k}}^\dagger-\sigma_{\mathbf{k}}^* b_{\mathbf{k}})\right], \quad \text{(B6)}$$

where we have set $\sigma_{\mathbf{k}}\equiv g_{\mathbf{k}}\varphi_{\omega_k}(t)\Sigma_m(i_m-j_m)\exp(-i\mathbf{k}\cdot\mathbf{r}_m)$. From the above equation, note that the first two exponential terms commute, hence we only have to take the trace over the third term. By doing this (see, e.g., Ref. [29]), we obtain the result

$$\mathrm{Tr}_B\left[\rho^B(0)\exp\left\{\sum_{\mathbf{k}}(\sigma_{\mathbf{k}}b_{\mathbf{k}}^\dagger-\sigma_{\mathbf{k}}^* b_{\mathbf{k}})\right\}\right] =\prod_{\mathbf{k}}\exp\left[-|g_{\mathbf{k}}|^2\frac{1-\cos(\omega_k t)}{(\hbar\omega_k)^2}\coth\left(\frac{\hbar\omega_k}{2k_B T}\right) \times\sum_{m,n}(i_m-j_m)(i_n-j_n)\cos\mathbf{k}\cdot\mathbf{r}_{mn}\right], \quad \text{(B7)}$$

from where Eq. (11) arises immediately.

[1] W. H. Zurek, Phys. Today **44**(10), 36 (1991).

[2] J. Preskill, Proc. R. Soc. London, Ser. A **452**, 567 (1998).

[3] N. H. Bonadeo *et al.*, Science **282**, 1473 (1998).

[4] C. P. Slichter, *Principles of Magnetic Resonance* (Springer Verlag, Berlin, 1996).

[5] P. W. Shor, in *Proceedings of the 35th Annual Symposium on the Foundations of Computer Science*, edited by S. Goldwasser (IEEE Computer Society Press, Los Alamitos, CA, 1994), p. 124.

[6] J. I. Cirac and P. Zoller, Nature (London) **404**, 579 (2000); Phys. Rev. Lett. **74**, 4091 (1995); C. Monroe *et al.*, *ibid.* **75**, 4714 (1995); K. Molmer and A. Sorensen, *ibid.* **82**, 1835 (1999); C. A. Sackett *et al.*, Nature (London) **393**, 133 (2000).

[7] N. A. Gershenfeld and I. L. Chuang, Science **275**, 350 (1997); D. G. Cory *et al.*, Proc. Natl. Acad. Sci. U.S.A. **94**, 1634 (1997); E. Knill *et al.*, Phys. Rev. A **57**, 3348 (1998); J. A. Jones *et al.*, Nature (London) **393**, 344 (1998); B. E. Kane, *ibid.* **393**, 133 (1998).

[8] Q. A. Turchette *et al.*, Phys. Rev. Lett. **75**, 4710 (1995); A. Imamoglu *et al.*, *ibid.* **83**, 4204 (1999); A. Rauschenbeutel *et al.*, *ibid.* **83**, 5166 (1999).

[9] A. Shnirman *et al.*, Phys. Rev. Lett. **79**, 2371 (1997); D. V. Averin, Solid State Commun. **105**, 659 (1998); Y. Makhlin *et al.*, Nature (London) **398**, 305 (1999); Y. Nakamura *et al.*, *ibid.* **398**, 786 (1999); C. H. van der Wal *et al.*, Science **290**, 773 (2000).

[10] A. Barenco *et al.*, Phys. Rev. Lett. **74**, 4083 (1995); D. Loss and D. P. DiVincenzo, Phys. Rev. A **57**, 120 (1998); G. Burkard *et al.*, Phys. Rev. B **59**, 2070 (1999); L. Quiroga and N. F. Johnson, Phys. Rev. Lett. **83**, 2270 (1999); J. H. Reina *et al.*, Phys. Rev. A **62**, 012305 (2000); J. H. Reina *et al.*, Phys. Rev. B **62**, R2267 (2000); F. Troiani *et al.*, *ibid.* **62**, R2263 (2000); E. Biolatti *et al.*, Phys. Rev. Lett. **85**, 5647 (2000).

[11] P. W. Shor, Phys. Rev. A **52**, R2493 (1995); A. M. Steane, Phys. Rev. Lett. **77**, 793 (1996).

[12] E. Knill and R. Laflamme, Phys. Rev. A **55**, 900 (1997).

[13] P. Zanardi and M. Rasetti, Phys. Rev. Lett. **79**, 3306 (1997); L.-M. Duan and G.-C. Guo, *ibid.* **79**, 1953 (1997); D. A. Lidar *et al.*, *ibid.* **81**, 2594 (1998).

[14] A. Beige *et al.*, Phys. Rev. Lett. **85**, 1762 (2000).

[15] J. Kempe *et al.*, Phys. Rev. A **63**, 042307 (2001), and references therein.

[16] L. Viola, E. Knill, and S. Lloyd, Phys. Rev. Lett. **85**, 3520 (2000); **82**, 2417 (1999); L. Viola and S. Lloyd, Phys. Rev. A **58**, 2733 (1998).

[17] G. S. Agarwal *et al.*, Phys. Rev. Lett. **86**, 4271 (2001), and references therein; G. S. Agarwal, Phys. Rev. A **61**, 013809 (2000); C. Search and P. R. Berman, Phys. Rev. Lett. **85**, 2272 (2000).

[18] D. Kielpinski *et al.*, Science **291**, 1013 (2001).

[19] P. G. Kwiat *et al.*, Science **290**, 498 (2000).

[20] G. M. Palma, K.-A. Suominen, and A. K. Ekert, Proc. R. Soc. London, Ser. A **452**, 567 (1996).

[21] L.-M. Duan and G.-C. Guo, Phys. Rev. A **57**, 737 (1998).

[22] A. J. Leggett *et al.*, Rev. Mod. Phys. **59**, 1 (1987).

[23] If relaxation mechanisms are also considered, in general $J_x^n, J_y^n \neq 0$. The presence of distinct error generators along *x*, *y*, and *z* make the noise processes non-Abelian and the Hamiltonian can no longer be solved analytically.

[24] This factorizable condition is the one that has been extensively studied so far. However, more general situations have been analyzed in connection with the influence functional path-integral method of Feynman and Vernon. See, e.g., Ref. [28].

[25] Formally, noise processes can be characterized in terms of the interaction algebra that they generate, see, e.g., Refs. [26,27].

[26] E. Knill, R. Laflamme, and L. Viola, Phys. Rev. Lett. **84**, 2525 (2000).

[27] P. Zanardi, Phys. Rev. A **63**, 012301 (2001), and references therein.

[28] C. Morais Smith and A. O. Caldeira, Phys. Rev. A **41**, 3103 (1990) and references therein; **36**, 3509 (1987); V. Hakim and V. Ambegaokar, *ibid.* **32**, 423 (1985).

[29] C. W. Gardiner and P. Zoller, *Quantum Noise* (Springer Verlag, Berlin, 2000).

[30] B. L. Hu, J. P. Paz, and Y. Zhang, Phys. Rev. D **45**, 2843 (1992).
[31] J. H. Reina, L. Quiroga, and N. F. Johnson (to be published).
[32] W. G. Unruh, Phys. Rev. A **51**, 992 (1995).
[33] Over the time scale considered for curve (a) in Fig. 7(i), the vacuum fluctuation plot overlaps with curve (b), obscuring it from view. The same happens with the vacuum fluctuation contribution associated with curve (b): this gets superposed with curve (c) and neither can be directly observed in Fig. 7(i).
[34] G. D. Mahan, *Many-Particle Physics*, 2nd ed. (Plenum, New York, 1990), p. 314.